# COMPARISON OF FULL-SCALE XV-15 BLADE-VORTEX INTERACTION NOISE CALCULATIONS WITH WIND TUNNEL DATA

Cahit Kitaplioglu and Wayne Johnson

*Army/NASA Rotorcraft Division*
*NASA Ames Research Center*
*Moffett Field, California*

Results from the TRAC acoustic prediction system were correlated with data from a test of an isolated full-scale XV-15 rotor in the NASA Ames 80- by 120-Foot Wind Tunnel. The airloads calculation provided by the original CAMRAD.Mod1 code in the standard TRAC system was exercised with several high resolution options, including the FPXBVI CFD code. In addition, the more recent CAMRAD II code was run in place of the original CAMRAD.Mod1. The CAMRAD II code, with a multiple trailer wake model yielding airloads at 3 degree azimuthal resolution, provided excellent correlation with measured BVI pulse amplitude, but less so for pulsewidth. There is indication that better results may be obtained with higher resolution airloads.

## Notation·

| | |
|---|---|
| c | speed of sound |
| $C_T$ | rotor thrust coefficient (shaft axes) |
| $M_{tip}$ | blade tip Mach number |
| r/R | microphone radial distance from hub |
| $r_{inner}$ | blade root cutout radius |
| R | blade radius |
| $\alpha_s$ | rotor shaft angle (positive aft) |
| $\beta_0$ , $\beta_{1c}$ , $\beta_{1s}$ | blade flap components |
| $\phi$ | microphone elevation angle (positive down from rotor plane) |
| $\mu$ | advance ratio |
| $\rho$ | air density |
| $\sigma$ | rotor solidity |
| $\theta_0$ , $\theta_{1c}$ , $\theta_{1s}$ | blade pitch components |
| $\psi$ | azimuth angle (positive conterclockwise from downstream) |

·*Presented at the American Helicopter Society International Technical Specialist Meeting On Aerodynamics, Acoustics, and Test and Evaluation, San Francisco, CA, January 23-25, 2002.* 

## Introduction

Noise, particularly the impulsive type due to blade-vortex interactions (BVI), is a major determinant of the economic and military viability of all rotorcraft. The alleviation of noise has been a focus of substantial research and development efforts by NASA and U.S. rotorcraft industry in recent years. One aspect of this effort has been the intensive work undertaken to create a comprehensive prediction system to compute rotorcraft noise. The culmination of this work, if successful, would create a design tool of obvious value to the development of next generation rotorcraft. Significant progress has been made in recent years in improving the predictive ability of purely computational techniques in calculating rotorcraft noise.

Among several approaches, the Tilt-Rotor Aeroacoustic Code (TRAC) system (Ref. 1) was developed cooperatively by NASA and industry participants, specifically focused on prediction of the noise field of tilt-rotor aircraft.

The objective of the present work was to determine the extent to which the TRAC system could predict the noise field of a full-scale XV-15 aircraft, as measured during a test in the NASA Ames 80- by 120-Foot Wind Tunnel. The main focus was to evaluate the various options of the TRAC system. Similar correlations have been carried out for an XV-15 flight test (Ref. 2). The TRAC codes were run as delivered with no attempt to adjust or optimize any

# Report Documentation Page

*Form Approved*
*OMB No. 0704-0188*



| | | |
|---|---|---|
| 1. REPORT DATE<br>**2002** | 2. REPORT TYPE | 3. DATES COVERED<br>**00-00-2002 to 00-00-2002** |

| | |
|---|---|
| 4. TITLE AND SUBTITLE<br>**Comparison of Full-Scale XV-15 Blade-Vortex Interaction Noise Calculations with Wind Tunnel Data** | 5a. CONTRACT NUMBER |
| | 5b. GRANT NUMBER |
| | 5c. PROGRAM ELEMENT NUMBER |
| 6. AUTHOR(S) | 5d. PROJECT NUMBER |
| | 5e. TASK NUMBER |
| | 5f. WORK UNIT NUMBER |
| 7. PERFORMING ORGANIZATION NAME(S) AND ADDRESS(ES)<br>**Army/NASA Rotorcraft Division,Army Aviation and Missile Command,Aeroflightdynamics Directorate (AMRDEC), Ames Research Center,Moffett Field,CA,94035** | 8. PERFORMING ORGANIZATION REPORT NUMBER |
| 9. SPONSORING/MONITORING AGENCY NAME(S) AND ADDRESS(ES) | 10. SPONSOR/MONITOR’S ACRONYM(S) |
| | 11. SPONSOR/MONITOR’S REPORT NUMBER(S) |

12. DISTRIBUTION/AVAILABILITY STATEMENT
**Approved for public release; distribution unlimited**

13. SUPPLEMENTARY NOTES
**Presented at the American Helicopter Society International Technical Specialist Meeting On Aerodynamics, Acoustics, and Test and Evaluation, San Francisco, CA, January 23-25, 2002**

14. ABSTRACT

15. SUBJECT TERMS

| 16. SECURITY CLASSIFICATION OF: | | | 17. LIMITATION OF ABSTRACT | 18. NUMBER OF PAGES | 19a. NAME OF RESPONSIBLE PERSON |
|---|---|---|---|---|---|
| a. REPORT<br>**unclassified** | b. ABSTRACT<br>**unclassified** | c. THIS PAGE<br>**unclassified** | **Same as Report (SAR)** | **10** | |

parameters, except those pertaining to rotor operating conditions.

This paper will briefly describe the existing TRAC system, CAMRAD II comprehensive code, the XV-15 wind tunnel test, and present comparisons between the data and computations.

## Code Description

The TRAC system is a framework for executing a series of computer codes that calculate, for a specified operating condition, rotor dynamics and aerodynamics, blade pressure distributions, and the resulting acoustic field. Presently, the components of the TRAC system include the CAMRAD.Mod1 code for comprehensive rotor dynamics/aerodynamics, the FPXBVI CFD code for blade aerodynamics, and the WOPMOD code for rotor acoustics (Fig. 1). It is important to note that other equivalent codes that serve similar purposes can be substituted in place of these components; TRAC merely provides a systematic methodology for defining the input/output and code execution format of the various codes. Thus, in the present work we were able to utilize the CAMRAD II code, in place of the CAMRAD.Mod1 module.

CAMRAD.Mod1 is based on the original CAMRAD code (Ref. 3) to perform a comprehensive performance, trim, and wake iterative analysis of the rotor. CAMRAD.Mod1, which provides only relatively coarse (10 deg) azimuthal resolution of blade loads, includes interfaces to higher resolution blade load calculations. One is the HIRES option that uses a high resolution reconstruction of the blade and wake positions from the far-wake influence coefficients. The near-wake is accounted for by a lattice model and airloads analysis. An alternative for accounting for the near wake is a post-processor (IPP) that utilizes indicial aerodynamic functions (Ref. 4). Both these techniques can yield compact section loading information at resolutions as small as 0.5 deg.

Another interface allows use of the FPXBVI CFD code (Ref. 5) for full surface loading distribution calculations at high resolution. FPXBVI evolved from the Full-Potential Rotor (FPR) CFD aerodynamics code with the addition of BVI analysis capability.

CAMRAD II is described in Reference 6. Whereas the original CAMRAD is based on a modal analysis of the blade, CAMRAD II is based on a finite element method and multibody dynamics and, thus, allows the analysis to more accurately model both the rotor and the overall vehicle. Furthermore, CAMRAD II includes more refined unsteady aerodynamic models and a robust free wake model to calculate the rotor nonuniform induced-velocities, using second-order lifting line theory and free wake geometry. Several wake models appropriate for tiltrotors are described in detail in Reference 7. Of these, the multiple- trailer wake model with consolidation in compression form (herein referred to simply as the multiple-trailer wake model) was found to yield the best results. The multiple-trailer wake model has a discrete trailed vortex line emanating from each of the blade aerodynamic panel edges. The calculation of the free wake geometry includes the distortion of all trailed lines, but because of the low spanwise resolution and the absence of viscous effects, a highly concentrated tip vortex is not produced. So a simulation of the tip vortex formation process (consolidation) is used. With the consolidation model, the trailed lines at the wing panel edges are combined into rolled-up vortices, using the trailed vorticity moment to scale the rate of rollup. All the vorticity in adjacent lines that have the same sign (bound circulation increasing or decreasing) eventually rolls up into a single vortex, located at the centroid of the original vorticity distribution. Using this model, there is good correlation of the calculated power and airloads with tiltrotor measurements (Ref. 7). For this paper, results are presented for the multiple-trailer wake model as well as for the rolled-up wake model, which features a fully developed tip vortex (and an inboard vortex when there is negative loading of the blade tip). With the rolled-up wake model (which is similar to the models that have been developed for helicopter rotors), good performance correlation is achieved for tiltrotors, but the calculated airloads are not accurate. The differences in the wake patterns produced by the rolled-up and multiple-trailer wake models are illustrated in Figure 2. For high-resolution results, the airloads are calculated using an azimuthal resolution of 3 deg. These high resolution results are produced by first obtaining the equilibrium solution of the coupled aerodynamic, wake, structural, and inertial problem at 15 deg azimuthal resolution, and then evaluating the airloads at 3 deg resolution using the blade motion from the 15 deg solution.

The WOPMOD code, based on the original WOPWOP code (Ref. 8), computes the far acoustic field at specified observer locations based on the rotor state and geometry, and the high resolution blade loads provided by HIRES, IPP, or FPXBVI. WOPWOP is an implementation of Farassat's time domain representation of the Ffowcs Williams/Hawkings aeroacoustic equation, excluding the quadrupole terms.

## Test Description

The experimental data used in the present correlation work were obtained during a test of a full-scale, isolated XV-15 rotor in the NASA Ames 80- by 120-Foot Wind Tunnel (Fig. 3). The test was described in detail in References 9 and 10. The rotor loads were measured using a six-component internal balance. There were no

measurements of the blade surface pressure distributions. Direct measurements of blade pitch, flapping, and lead-lag were available. The acoustic field was measured using four moving microphones (Mics #1-4) to obtain the noise footprint under the advancing side of the rotor (Fig. 4). There was also a fixed microphone in the right/forward quadrant at the estimated peak BVI directivity location (Mic #5). The acoustic data were recorded at a rate of 2048 samples per revolution for 16 rotor revolutions. The measured acoustic data were synchronously averaged to yield data of one revolution duration, as detailed in Reference 10. The wind tunnel data, in contrast to flight test data (Ref. 2), were quite steady and repeatable. The data used in this correlation study were not filtered (except for anti-alias filtering prior to digitization during data recording). The data, therefore, contain features arising from all noise mechanisms, including BVI, as well as from the presence of background noise and reflections.

A single test condition (Table 1) from this test, representing a high BVI noise case, was selected for this correlation work. The main results presented below are for the forward microphone (Mic #5: r/R=6, $\phi$=20 deg, $\psi$=150 deg). Some additional results are also shown for one of the traversing microphones (Mic #4: r/R=2.77, $\phi$=41 deg, $\psi$=136 deg). A more extensive study involving additional operating conditions and microphone positions was not attempted. The performance codes were run to match measured $C_T/\sigma$ and 1/rev flapping. The blade pitch components included in Table 1 are the experimentally measured values.

## Correlation Results

A total of seven computations, which include airloads and far-field acoustics, were performed, as enumerated in Table 2. The final acoustic results are shown in Figures 5 - 9 as Sound Pressure time histories per rotor revolution. A legend is included on each figure to indicate the calculation method, specified in the first column of Table 2. The line colors and types are consistent across the figures for ease of comparison. Only a portion of a rev, centered on the middle pulse, is shown for clarity. There were some blade-to-blade differences in the data. The middle pulse is representative of the other two. The time axes of the data were shifted by a small amount (equivalent to approximately 3.5 deg of azimuth) to correct for an error in setting the azimuth reference during testing.

Initially the standard TRAC code was executed without the HIRES option. This is not recommended practice. It was done to establish a reference for evaluating subsequent calculations using higher resolution airloads.

The TRAC code was rerun with the HIRES and IPP options active. The results (Fig. 5) indicate that, as expected, low resolution airloads are clearly inadequate to capture the main features of BVI acoustics. The airloads provided by the high-resolution, near-wake, indicial aerodynamics improve the situation somewhat. However, it is the airloads generated by the HIRES internal near-wake model, at 0.5 deg azimuthal resolution, that begin to show reasonable correlation with the experimental data. The measured waveform has a roughly double-N shape with a very prominent positive central peak and two lesser side peaks. The CAMRAD.Mod1/HIRES computation captures the general wave shape; however, it underpredicts the peak amplitude of the main pulse by approximately 30 percent. The trailing edge of the computed waveform (the right lesser peak of the data) contains a local fluctuation not evident in the data. The pulsewidth of the computed main pulse is narrower than the data by approximately 25 percent.

The result of using the FPXBVI code to provide full surface airloads at 1 deg azimuthal resolution is shown in Figure 6. The correlation with data is comparable with that for the HIRES computation. The main pulse peak amplitude is slightly less than the HIRES computation, as is the peak-to-peak value. On the other hand, the pulsewidth exactly matches that of the data.

The TRAC system was also executed with the CAMRAD II code substituted in place of CAMRAD.Mod1. At an azimuthal resolution of 10 deg for the airloads calculations, the results using the multiple trailer wake model were comparable to those of low resolution CAMRAD.Mod1 (Fig. 7). At a finer resolution of 3 deg, results were highly dependent on the wake model. Some improvement, but still unsatisfactory, correlation with data was obtained using the rolled-up wake model. The multiple trailer wake model, on the other hand, yielded good correlation with data as indicated in Figure 7. The peak value of the BVI sound pulse is well predicted, as is its general shape. However, the two side peaks are hardly evident in the computation. The computed pulsewidth is approximately double that of the data. Unfortunately, even finer resolution airload calculations could not be performed due to memory limitations. However, the trend appears to be toward improved results. It remains to be seen whether with 1 or 0.5 deg resolution airloads, both the double peaks as well as the pulsewidth may be better predicted.

A summary plot showing the results from the three best code combinations is shown in Figure 8.

Computations for the other microphones yielded similar results, as illustrated for Mic #4 in Figure 9. Note the different vertical scale as well as the phase shift of the BVI pulse from the previous figures for Mic #5, due to the closer position of this microphone. In this particular

case, the CAMRAD.Mod1/HIRES method overpredicts the BVI sound pulse amplitude.

Correlation results for XV-15 flight tests (Ref. 2) are comparable, for the main BVI pulse due to the dominant rotor, to those obtained in the present study, using the CAMRAD.Mod1/HIRES method in both cases. Yet, in using data from a wind tunnel test, rather than a flight test, uncertainty in operating conditions is largely eliminated.

## Conclusions

Calculated BVI noise signatures for a full-scale tiltrotor were compared to wind tunnel data. Several variants of the TRAC acoustic prediction system were correlated with data from a test of an isolated full-scale XV-15 rotor. The original CAMRAD.Mod1 code yields acceptable results with an airloads computation at a high azimuthal resolution of 0.5 degree. Airloads computed using the FPXBVI code at 1 degree resolution yields comparable results. The CAMRAD II code, with a multiple trailer wake model yielding airloads at 3 degree azimuthal resolution, provided the best correlation with respect to BVI pulse amplitude, but missed some features of the measured waveform, as well as the pulsewidth. The trend appears to be toward improving results with airloads computed at higher resolutions.

## References

1. Boyd, Jr., D.D., Brooks, T.F., Burley, C.L., Jolly, Jr., J.R., “Aeroacoustic Codes for Rotor Harmonic and BVI Noise – CAMRAD.Mod1/HIRES: Methodology and User’s Manual,” NASA TM 110297, March 1998.

2. Boyd, Jr., D.D., Burley, C.L., “Analysis of Measured and Predicted Acoustics from an XV-15 Flight Test,” American Helicopter Society 57$^{th}$ Annual Forum, Washington, DC, May 2001.

3. Johnson, W., “A Comprehensive Analytical Model of Rotorcraft Aerodynamics and Dynamics,” NASA TM 81182, June 1980.

4. Beddoes, T.S., “Two and Three Dimensional Indicial Methods for Rotor Dynamic Airloads,” American Helicopter Society Specialists’ Meeting on Rotorcraft Dynamics, Dallas, TX, November 1989.

5. Bridgeman, J.O., Prichard, D., Caradonna, F.X., “The Development of a CFD Potential Method for the Analysis of Tilt-Rotors,” American Helicopter Society Technical Specialists’ Meeting on Rotorcraft Acoustics and Fluid Dynamics, Philadelphia, PA, October 1991.

6. Johnson, W. "CAMRAD II, Comprehensive Analytical Model of Rotorcraft Aerodynamics and Dynamics." Johnson Aeronautics, Palo Alto, California, 1992-2002.

7. Johnson, W. "Influence of Wake Models on Calculated Tiltrotor Aerodynamics." American Helicopter Society International Technical Specialists Meeting On Aerodynamics, Acoustics, and Test and Evaluation, San Francisco, California, January 2002.

8. Brentner, K.S., “Prediction of Helicopter Rotor Discrete Frequency Noise,” NASA TM 87721, October 1986.

9. Kitaplioglu, C., Acree, C.W., Light, J.S., “XV-15 Aeroacoustic Testing at NASA Ames Research Center,” *Journal of the American Helicopter Society*, Vol. 45, No. 3, July 2000.

10. Kitaplioglu, C., “Blade-Vortex Interaction Noise of a Full-Scale XV-15 Rotor Tested in the NASA Ames 80-by 120-Foot Wind Tunnel,” NASA TM 208789, July 1999.

Table 1. Rotor Operating Parameters

| Parameter | Value |
|---|---|
| RPM | 584.8 |
| $M_{tip}$ | 0.686 |
| $\mu$ | 0.170 |
| $\alpha_s$ | 4.0° |
| c | 340.29 m/sec |
| $\rho$ | 1.226 $Kg/m^3$ |
| $r_{inner}$ | 0.877 m |
| R | 3.81 m |
| $\theta_0$ | 4.25° |
| $\theta_{1c}$ | 1.09° |
| $\theta_{1s}$ | -2.06° |
| $\beta_0$ | 1.65° |
| $\beta_{1c}$ | 0° |
| $\beta_{1s}$ | 0° |
| $C_T/\sigma$ | 0.0758 |

Table 2. Computation Methods

| Method | Description | Azimuthal resolution of calculated airloads (deg) |
|---|---|---|
| 1 (LORES) | Camrad.Mod1 (low res) + WOPMOD (not recommended; included for reference) | 10.0 |
| 2 (HIRES) | Camrad.Mod1/HiRes + WOPMOD | 0.5 |
| 3 (HIRES+IPP) | Camrad.Mod1/HiRes + IPP + WOPMOD | 0.5 |
| 4 (HIRES+FPX) | Camrad.Mod1/HiRes + FPXBVI + WOPMOD | 1.0 |
| 5 (2LORES) | Camrad II (low res) + WOPMOD | 10.0 |
| 6 (2HIRES/ROLL) | Camrad II (hi res, rolled-up wake) + WOPMOD | 3.0 |
| 7 (2HIRES/MULT) | Camrad II (hi res, multiple trailer wake) + WOPMOD | 3.0 |

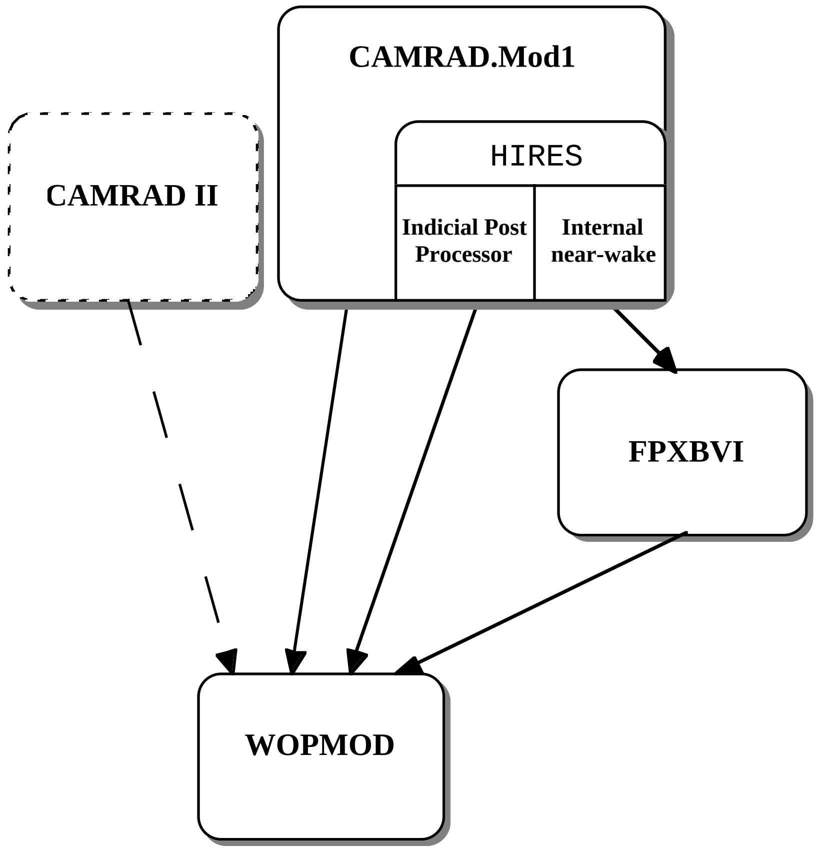


**Fig. 1. Schematic of the TRAC system**

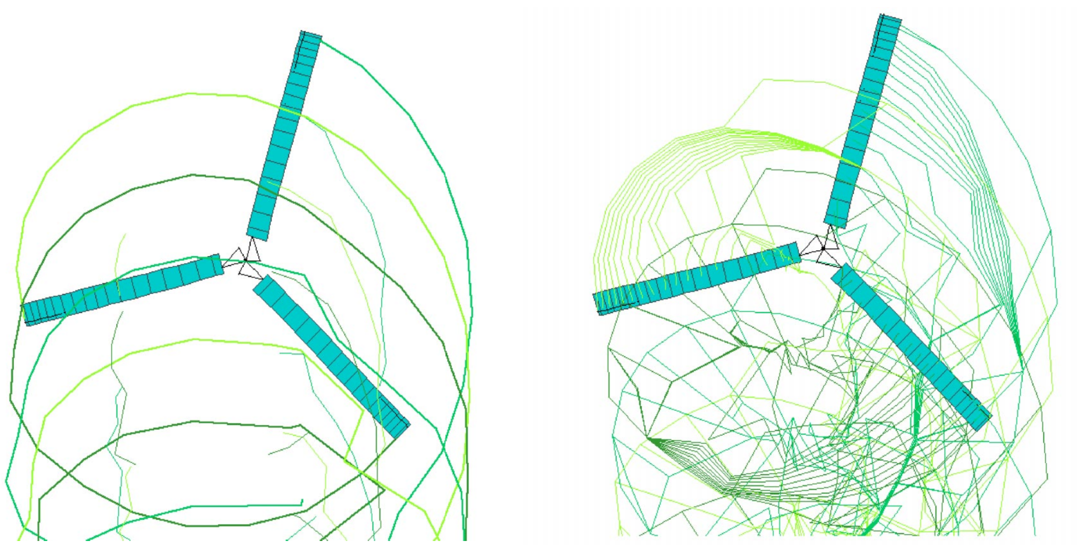

(a) Rolled-up wake

(b) Multiple-trailer wake with consolidation, compression form

**Fig. 2. Two wake models in CAMRAD II computations.**

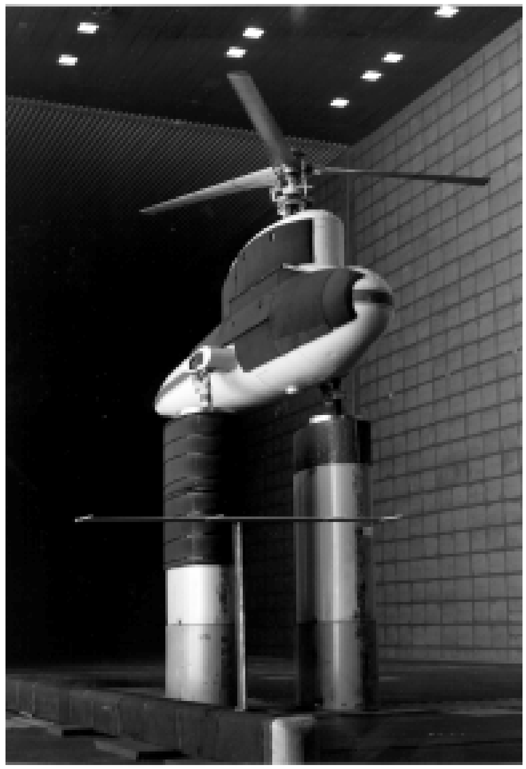

**Fig. 3. The XV–15 right-hand rotor mounted in the 80- by 120-Foot Wind Tunnel.**

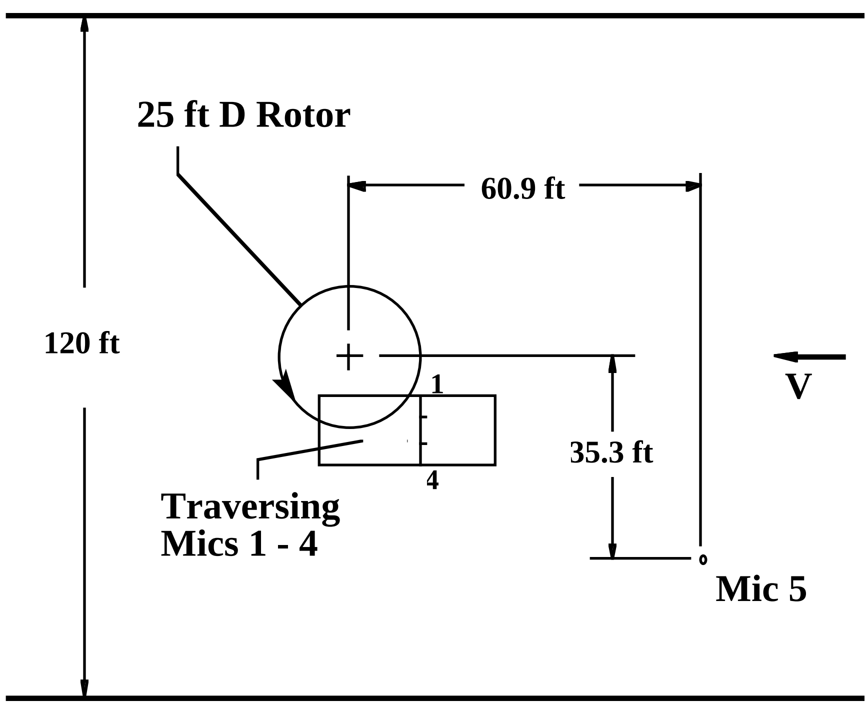


**Fig. 4. Schematic of microphone positions for the XV-15 test in the NASA Ames 80- by 120- Foot Wind Tunnel.**

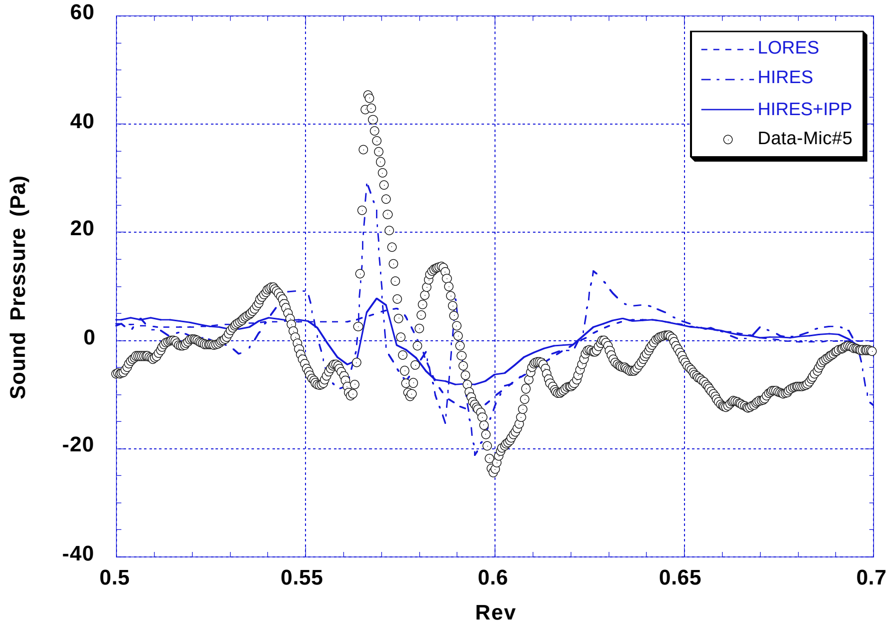


**Fig. 5. Comparison of CAMRAD.Mod1 results with data.**

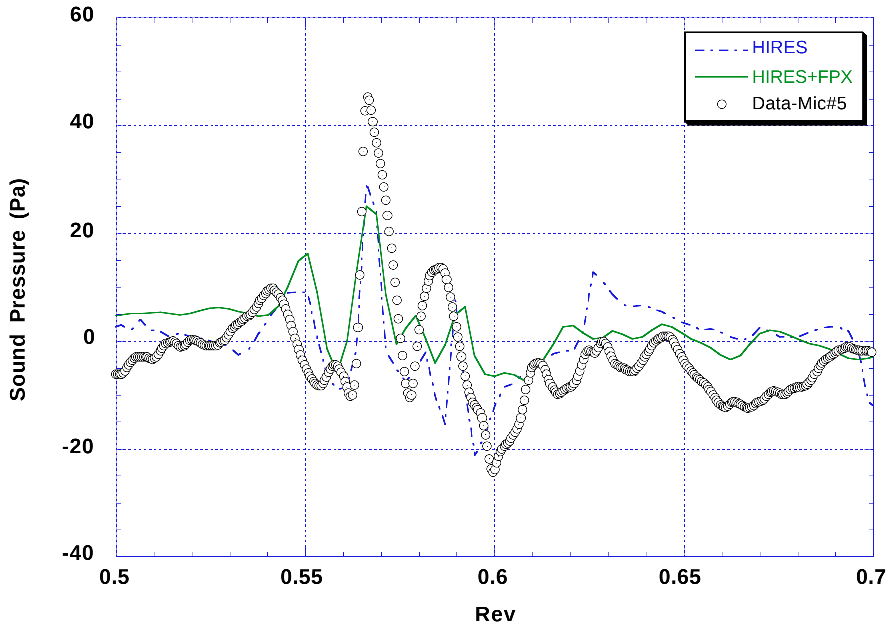


**Fig. 6. Comparison of CAMRAD.Mod1/HIRES and FPXBVI results with data.**

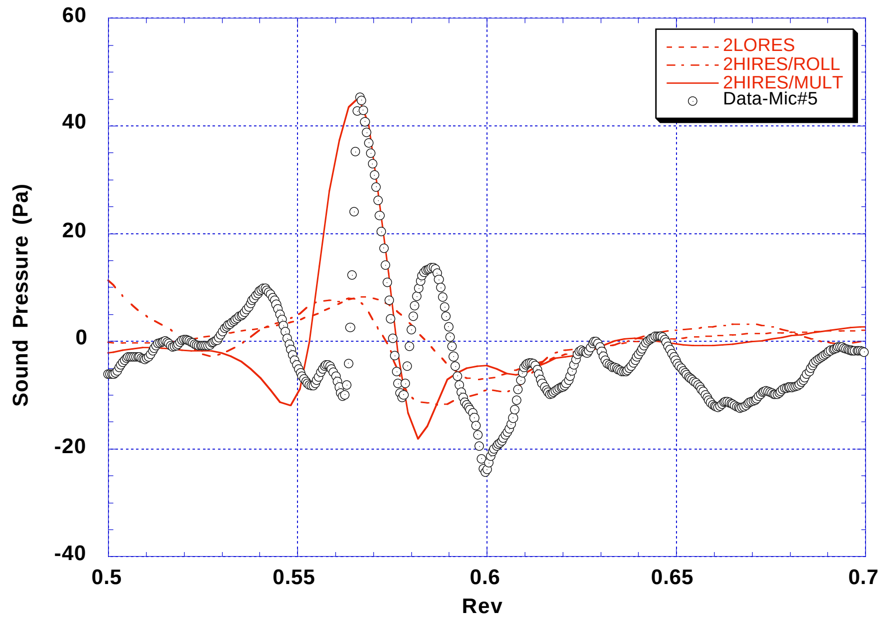


**Fig. 7. Comparison of CAMRAD II results with data.**

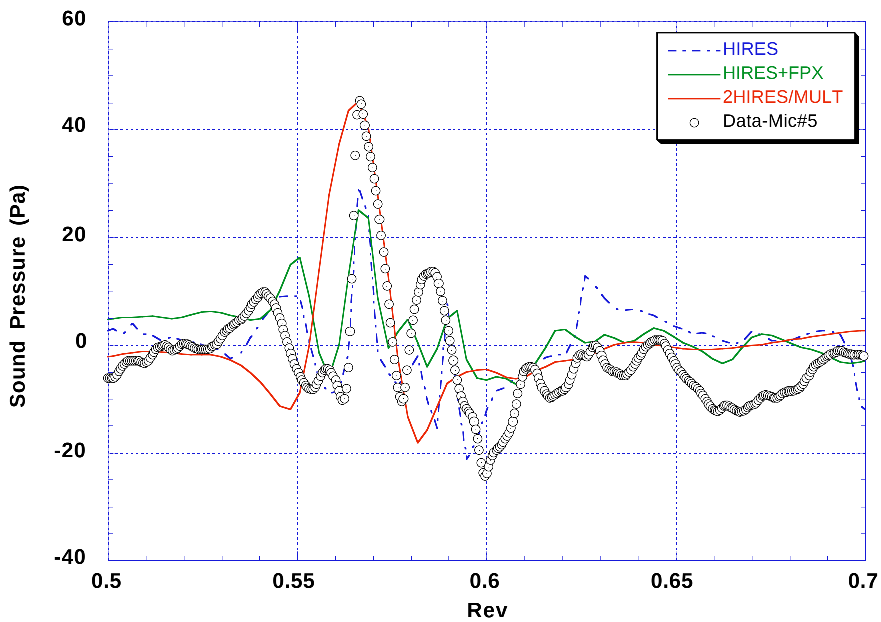


**Fig. 8. Summary of main results; comparison of best CAMRAD.Mod1 and CAMRAD II results with data. Mic #5.**

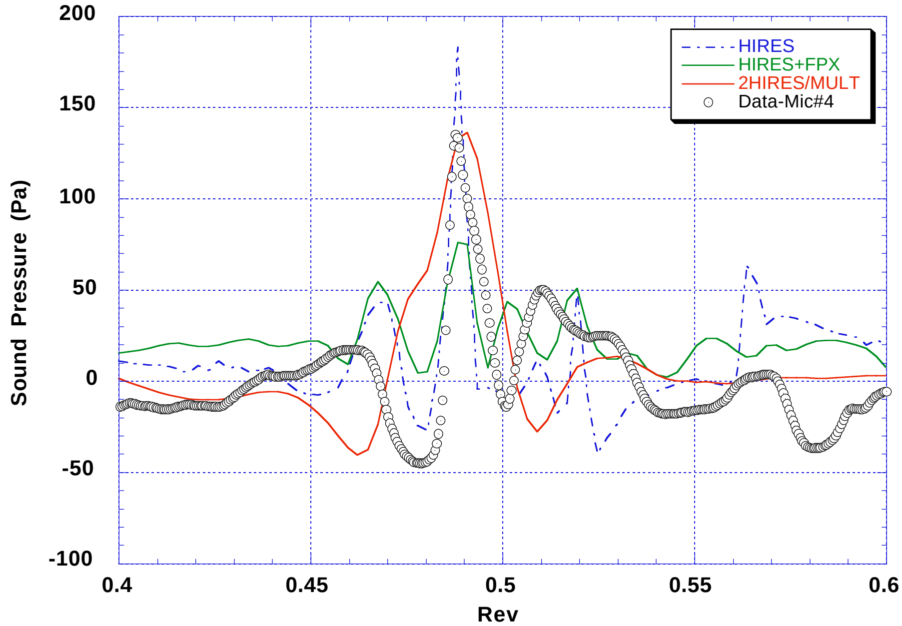


**Fig. 9. Summary of results; comparison of best CAMRAD.Mod1 and CAMRAD II results with data. Mic #4.**